Journal of Visualization, Vol. 11, No. 2 (2008)153-162

**Regular Paper**

# Near–Field Acoustic Characteristics of Screech Jet Exhausted from a Nozzle with a Hard Reflecting Plate

Nakazono, Y.*[1] , Sonoda, Y. *[2], Ouchi, Y. *[3] and Nasu, Y. *[4]

*1 Department of Mechanical Systems Engineering, School of Engineering, Kyushu Tokai University
9-1-1 Toroku, Kumamoto, Japan. E-mail: ynakazon@ktmail.ktokai-u.ac.jp
*2 Industrial Techno-Research Institute, Kyushu Tokai University
*3 Department of Information Systems Engineering, Kyushu Tokai University
*4 Graduate School of Engineering, Kyushu Tokai University

Received 19 July 2007
Revised 28 November 2007

***Abstract*** : The standing wave in the near field of the screech jet exhausted from a nozzle with a hard plate works on the jet flow as the forcing wave by the location of a reflecting plate, and then jet flow is considered to be changed. Moreover, the reflector location from the nozzle changes the sound pressure contours of the near field. Intensity maps of the screech tone which indicate the propagation to the jet axial direction or the radial direction of the jet by the presence of the reflector plate have not been explored. In the present paper, acoustic characteristics in the near field of the screech tone with the reflecting plate are studied using an optical wave microphone, which can measure the sound propagating for both vertical and horizontal directions to the jet axis. As a result, the standing wave in the near field of the screech jet with the reflector has two types: One is the standing wave between the hydrodynamic pressure fluctuation propagating jet downstream and the sound pressure propagating upstream, and the other is the standing wave by the difference between the wavelength of the sound wave and the wavelength at the place close to the jet.

***Keywords*** : Screech jet, Hard reflecting plate, Near-field, Standing wave, Optical wave microphone, Shadowgraph.

## 1. Introduction

In practical supersonic jet engines, the circumference of the engine has reflective airframe surfaces, and the occurrence of fatigue failure of aircraft structures is possible on such surfaces exposed to powerful screech tones for a long period. Moreover, a common experimental facility has a flange, acting as a reflector, at the exit of a plenum chamber connected to the nozzle. The details of the reflector's influence on the sound field during screech have remained unsolved.

The acoustic characteristics of screech jet tones with a reflecting plate to reduce the upstream propagating noise have been studied by many researchers. Powell (1953), who is the pioneer of screech jets, stated that the reflective surface in the nozzle exit influences the screech tone sufficiently. Harper-Bourne and Fisher (1974) first mentioned that the reflector surface at the jet exit made the screech steady, but that it also made the screech dominant. Moreover, they found that covering the reflector with absorbing acoustic foam reduces the screech tone. Nagel (1983) noted that when the reflector was located at odd multiples of $\lambda/4$ ($\lambda$:wavelength) from the nozzle exit, the screech tone was minimized. Norum (1983) studied the effect of reflector size and its surface on the

screech production, and he also indicated that the reduction of screech tone upstream due to shielding increased the broadband shock noise over most operating conditions. The above mentioned research was carried out in the far-field measurement for the screech jet.

The standing pattern in the near field of screeching jets without the reflector was reported by Westley and Woolley (1975), Rice and Taghavi (1992) and Panda (1999). Panda also reported the physical meaning for the screech frequency of screeching jets.

However, the effect of the reflector on the near acoustic field of the screech jet has never been obvious. The standing wave in the near field of the screech jet with a hard plate works on the jet flow as the forcing wave by the location of the reflecting plate, and then the jet flow is considered to be changed. Moreover, the reflector location from the nozzle changes the sound pressure contours of the near field. Intensity maps of the screech tone which indicate the propagation to the jet axial direction or the radial direction of the jet by the presence of the reflector plate have not been explored.

In the present paper, the acoustic characteristics in the near field of the screech tone with the reflecting plate are studied using an optical wave microphone (other name: opt-microphone), which can measure the sound propagating for both vertical and horizontal directions to the jet axis.

## 2. Experimental Apparatus and Method

The measurement of both the acoustic and flow characteristics was carried out in a semi-anechoic room (size: 6.4 m × 4.6 m × 2.5 m). After air flow supplied with a compressor was passed through a muffler to reduce the noise produced upstream, it entered a plenum chamber (180 mm inner diameter × 800 mm axial length), which had three 100-mech screens, and it was exhausted from a nozzle attached to the plenum chamber. The nozzle used in the present experiment is a tube nozzle extended with a straight length of 46 mm from a normal nozzle exit to the downstream and its inner diameter was 10 mm. Elongation of the straight section of the nozzle increases the thickness of the boundary layer (Ahuja, 1997). Therefore, it is considered that the acoustic characteristics of the screech tone for the tube nozzle differ from that for the normal nozzle. Non-dimensional screech frequencies ($fD_j/U_j$), which were measured with a condenser microphone at a distance of 600 mm from the nozzle exit and an observation angle of 120° from the downstream jet axis, as a function of Mach number $M_j$, are shown in Fig. 1, where f is screech frequency, $D_j$ effective nozzle diameter, $U_j$ fully expanded jet velocity, and $M_j$ fully expanded jet Mach number. Tam's theory (1984) is also shown in the figure. From the figure, it is found that the acoustic characteristics of the screech tone for the tube nozzle are similar to those for the normal nozzle, and the screech frequencies agree with the results of Tam's theory. The shape of the tube nozzle with the reflecting plate is shown in Fig. 2. A hard reflecting plate, which has a diameter of 200 mm, a thickness of 5 mm and is made of acrylic plastic, set on the circumference of the nozzle can move upstream of the nozzle exit. Nagel et al. (1983) and Norum (1983) reported that a reflector with a radius greater than one wavelength of the fundamental screech tone would be adequate in canceling the screech. Our reflector radius is 100 mm, which is about 3 times larger than the longest wavelength forecasted in this study. Therefore, our reflector size satisfies the recommended reflector size.

Jet noise in the far field was measured with a 1/4 inch condenser microphone, which has a flat frequency characteristic until 120 kHz, located at 600 mm from the nozzle exit and 90° from the downstream jet axis. The obtained data was analyzed with a FFT analyzer. The reflector was moved to the upper-side from the nozzle at an interval of every 1mm. The sound pressure spectra were measured at each plate position of the reflector. The experiment was mainly conducted at a nozzle pressure ratio of 3.71, which is the ratio of the plenum chamber pressure to ambient pressure. The nozzle pressure ratio of 3.71 corresponds to the fully expanded jet Mach number of 1.51, which demonstrates the jet structure of the helical mode, as shown in Fig. 1.

From the far-field experiment, we chose a reflector-to-nozzle spacing L of 10 mm and 20 mm, which showed the maximum and minimum screech tone level respectively, for the acoustic measurement in the near field.

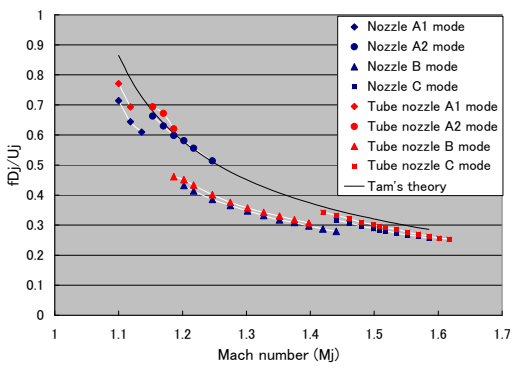


Fig. 1. Screech frequency as a function of Mach number.

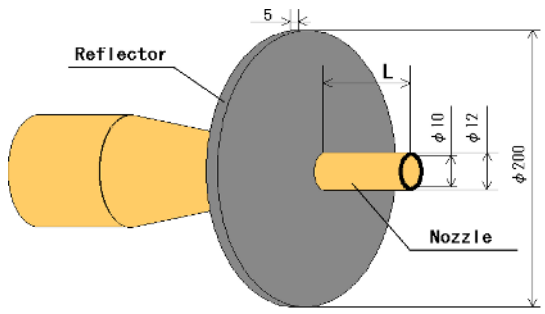


Fig. 2. Shape of tube nozzle with reflector.

# 3. Basic Characteristic of Opt-Microphone

The optical wave microphone has been studied by Sonoda (1994 and 2001) utilizing the far forward scattering (Evans, 1982 and 1983) or Fraunhofer diffraction (Sonoda,1983) methods, which were developed as a new means to measure long-wavelength plasma waves. From a view of fluid dynamic research, its fundamental techniques and application to the jet noise measurement have been studied by Nakazono (2002 and 2005).

In the present chapter, the principle and main results such as frequency characteristic and directivity of the opt-microphone are briefly described.

## *3.1 Principle of Opt-Microphone*

The principle of the opt-microphone is based on the wave-optical description of the effect of acoustic waves on the phase of a laser light injected in the sound field. This method is based on the Fraunhofer diffraction technique (Sonoda, 1994 and 2001), in which the definition of a laser beam is a little different from the far forward scattering, as shown in Fig. 3, where the incident laser beam is assumed to be of Gaussian type. When the incident probing laser beam crosses a sound wave, diffracted waves are generated by the density gradient of sound. Diffracted waves propagate in the penetrating beam through the Fourier optical system and reach the observing plane, which is set in the back focal plane of the receiving lens. The diffracted optical waves are homodyne-detected there by using the penetrating laser light as a local oscillating power. The multiple-diffraction effect or higher orders diffraction light could be neglected in the case of audio waves. The obtained optical intensity profiles include both the DC component and the diffracted AC component. The DC component is removed in the electric circuit and only the 1st AC component of the optical signal intensity is detected.

The spatial intensity of the resultant optical field at the back focal plane of a receiving lens is given by the following equation (Evans, 1982; Sonoda,1983),

$$I_{ac} = I_0 \Delta\phi_0 [\exp\{-(u^2+(u-\theta)^2)\}+\exp\{-(u^2+(u+\theta)^2)\}] \sin\omega_a t \quad (1)$$

where $I_0=(2P_0/\pi w_f^2)\exp[-2(y_f/w_f)^2]$ [W/m$^2$], $\Delta\phi = k_i(\mu_0 - 1)\Delta d\Delta p / \gamma p$, $\mu_0$ :refractive index of air, $\gamma$ :specific heat ratio, $\Delta d$ :width of sound, $p$ :atmospheric pressure, $\Delta p$ :sound pressure, $k_i$: wave number of laser light, $\omega_a$ : angular frequency of sound wave, $P_0$: laser power, $u = x_f/w_f$: the normalized x-coordinate in the back focal plane, $\theta = k_a w_0/2$: the normalized wave number, $k_a$: wave number of sound wave, $w_0$: radius of laser beam waist size in sound incident region, $w_f$, $x_f$, $y_f$: radius of the beam cross section, x-coordinate and y-coordinate in the observing plane, respectively.

Based on the above equations, numerical calculations of the diffraction pattern are carried out, in which a visible laser was assumed for the probing laser beam. Examples of spatial distributions of the intensity and the phase of the diffraction pattern are shown in Figs. 4(a) and (b). The spatial profile of the diffracted light pattern oscillating at the sound frequency has two peaks, the position of

which do not change with frequency in the audio-wave or the low frequency ultrasonic band. On the other hand, the temporal phase difference between the right and left diffraction patterns oscillating at $\omega_a$ is $\pi$, as shown in Fig. 4(b). From Eq. (1), it is found that the optical signal intensity is theoretically in proportion to the frequency of the sound wave. In application to jet noise measurement, the frequency response of the opt-microphone system is made flat over the whole frequency band by an electric signal processing circuit.

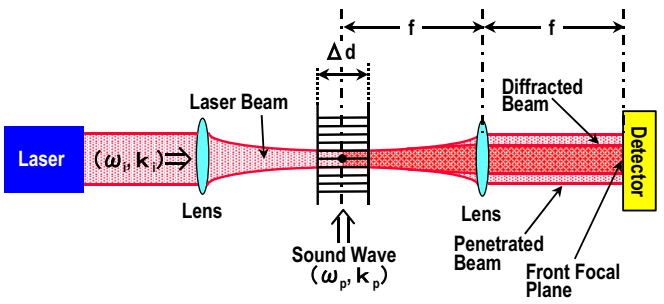


Fig. 3. Theorem figure of Fraunhofer diffraction method.

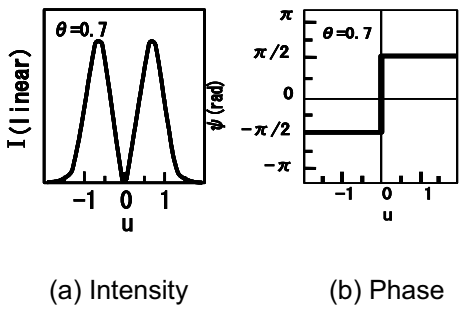


Fig. 4. Spatial distributions of the intensity and phase of the diffraction pattern.

### *3.2 Basic Characteristics*

A block diagram for the measurement is shown in Fig. 5. The experimental apparatus consists of a sound generation system, optical system, opt-detecting system and electric processing system. The experiment was carried out in a semi anechoic room. The laser is a diode laser with a circular beam (wavelength: 635 nm, normal power: 10 mW). The shape of the 1st, 2nd, 3rd, 4th and 5th lens is convex, convex-flat, flat-convex, convex and convex-flat, respectively. The optic detector is a silicone photodiode (size: 1.1 mm × 1.1 mm, detect sensitivity: 0.43A/W, equivalent noise power: $6.8 \times 10^{-16}$ W/Hz$^{1/2}$). Output voltage from a photo diode includes the signals of both an AC component and a DC component, and then only the AC component is produced with an electric filter circuit. In a sound generation system, a pure tone is generated with an oscillator by monitoring the frequency with a frequency counter instrument. After the pure tone is amplified with an audio amplifier, it is radiated from a tweeter (reproduction frequency response: 4 kHz to 45 kHz, diameter: 40 mm) located at a position of 60 mm below a laser beam. The output signal obtained by the opt-microphone is amplified by an amplifier and is read with a FFT analyzer, which is also calibrated by a condenser microphone.

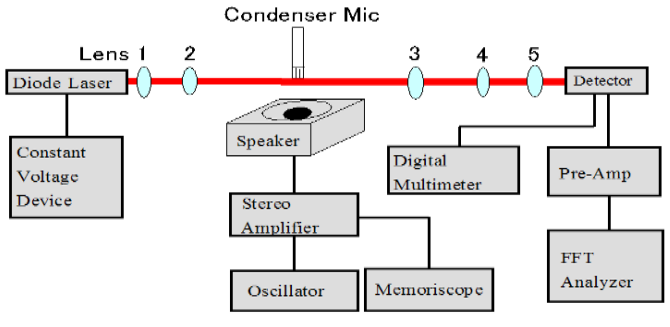


Fig. 5. Block diagram for measuring acoustic characteristics of opt-microphone.

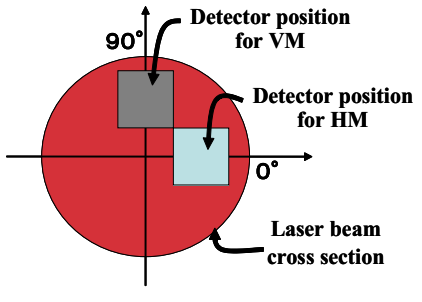


Fig. 6. Detector positions for VM and HM Measurements.

In the present measurement, the signal intensity obtained by the opt-microphone is called a laser signal intensity level (LIL), which is defined as $LIL(dB) = 90 + 20\log(V_{sig} / V(10kHz, 90dB))$, where V(10 kHz, 90 dB) means the output voltage for the radiated sound of 10 kHz and 90 dB, to distinguish the signal intensity from the sound pressure level (SPL) by the condenser microphone.

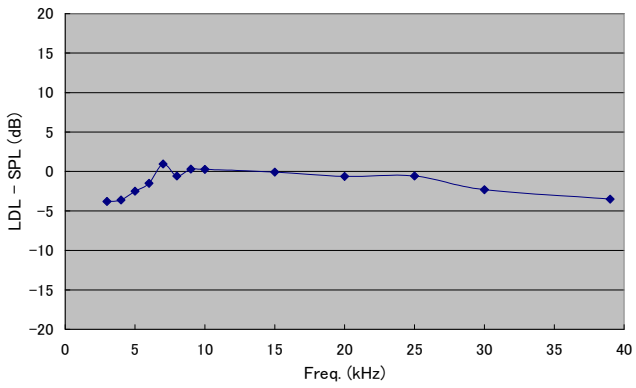


Fig. 7. Frequency properties of opt-microphone.

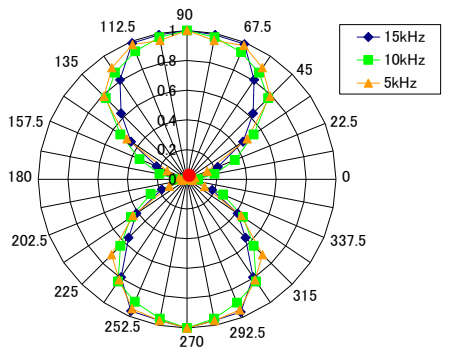


Fig. 8. Directivity of opt-microphone.

Figure 7 shows the frequency properties of the opt-microphone with an electronic signal processing circuit to make it flat, in which the ordinate is the difference between LIL and SPL and the calibration for the sound width is not performed. We can see that the acoustic frequency properties of the opt-microphone are constant until 30 kHz, and the difference of LIL to SPL is -3.5 dB at 39 kHz. On the other hand, the width of sound at 39 kHz is 36 mm (FWHM) and about two times narrower than 10 kHz and the effective difference at 39 kHz is estimated to be lower than +2.5 dB. The power spectra of jet noise in the present experiment has the dominant level above the frequency of 10 kHz, but the effect of the sound width has to be taken into account for the opt-microphone measurement.

Directivity in the plane perpendicular to the laser beam is shown in Fig. 8, in which the photo detector is set at the 90° line in Fig. 6. The small red circular symbol in the center of the figure shows the laser beam cross section. From Fig. 8, directivity shows 2 approximate circles on the vertical line. The sharp directivity is not found for all frequencies in the measured frequency range. The sound wave radiated from the horizontal is not detected in this configuration. Directivity of the opt-microphone is similar to that of the microphone of sound pressure gradient type. In this case, we call it “the measurement mode of the vertical direction component (abbreviated symbol: VM)”.

If we set the opt-microphone for the horizontal direction in the plane perpendicular to the laser beam, in which the photo detector is set at the 0° line in Fig. 6, 2 approximate circles on the horizontal line should be formed. This setting is called “the measurement mode of the horizontal direction component (abbreviated symbol: HM)”.

# 4. Acoustic Characteristics in the Near Field

The positions of the hard reflecting plate of L = 10 mm and 20 mm were chosen based on the acoustic measurement of the far-field mentioned above and their results were compared with that of the nozzle without reflector (other name: the plateless nozzle).

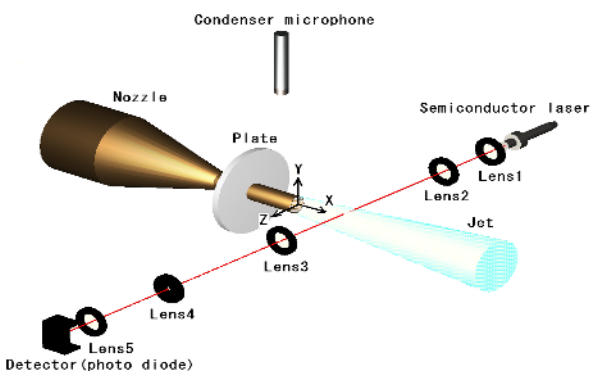


Fig. 9. Experimental apparatus of the jet and opt-microphone system.

### *4.1 Measuring Positions*

Figure 9 shows the opt-microphone system for measuring the near field of jet noise. In the case of the measurement of the X direction, the opt-microphone was moved at an interval of every 2 mm from the position of the reflector to X = 100 mm. In particular, at the positions of Y = 10 mm and 20 mm, the opt-microphone was moved at an interval of every 1 mm downstream to obtain the detailed distributions of the laser signal intensity level (LIL) in the near field. In the case of the Y direction, after measuring at the position of 7 mm from the jet center axis, it was moved at an interval of every 5mm within a range from 10 mm to 50 mm. The measurement was carried out at the places of about 790 points. At all positions, the power spectra of laser signal intensity were analyzed with the FFT analyzer, and the screech tone was extracted from the FFT data.

### *4.2 Results and Discussion*

Figure 10 shows the contours of laser signal intensity measured by VM and HM modes at a screech frequency of 12.5 kHz, and also a shadow-graph for the jet exhausted from the plateless nozzle. Yellow color is the strongest intensity and blue color the weakest intensity. As the minimum radial position of the laser beam is 7 mm from the jet center axis, the laser beam may pass through the jet in the downstream. When the laser beam passes through the jet, it is difficult for the opt-microphone to discriminate fluctuating pressure between the sound pressure and the hydro-dynamic pressure fluctuation. Intensity order of the hydro-dynamic pressure fluctuation is higher than the acoustic fluctuation. The hydro-dynamic pressure fluctuation decays exponentially away from the jet boundary (Morris, 1977; Ramsh, 2006), which causes the acoustic fluctuations to dominate after a certain radial distance. As the discrete frequencies in the power spectra of the laser signal intensity measured in the jet coincide that of the screech tone in the acoustic near field (Nakazono, 2002), some data on frequencies obtained in the both regions will be useful to study the relation between both pressure fluctuations.

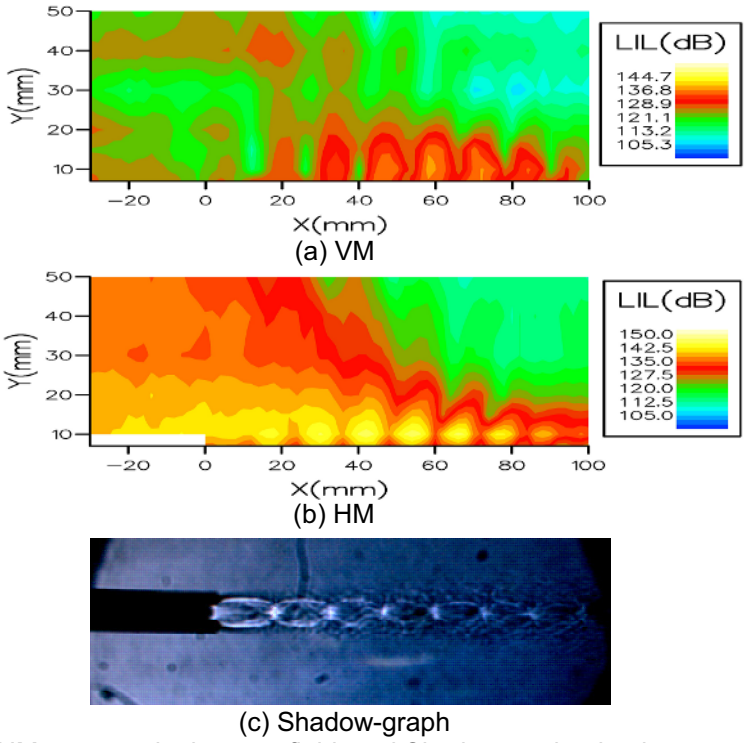


Fig. 10. VM and HM contours in the near field, and Shadowgraph, plateless nozzle, f = 12.5 kHz.

As the laser diffraction is proportional to the width of the acoustic field, the sound pressure obtained with opt-microphone may underestimate in the near field and overestimate in the far-field. In the present experiment, the effect of the width of the acoustic field was not corrected. However, even though not estimating the width of the acoustic field, it was found that the power spectra of the laser signal intensity at the location of (X,Y) = (0 mm, 50 mm) for the jet Mach number of 1.51 agree

with the sound pressure spectra with the condenser microphone (Nakazono et. al., 2006). The effect of the width of the acoustic field must study in detail hereafter.

From the figure in Fig. 10, it is found that the strongest noise source is placed near the 3rd and 4th shock locations, and the strongest screech tone propagates upstream. The results agree with those of previous research done by many researchers. From the HM mode, the screech tone radiates greatest at 180 degrees, and it decreases with the distance to the radial direction. The distance between the strongest optic intensities for the X direction is 12.3 mm, and this value corresponds to 0.82 times of the shock cell spacing of 15 mm, which is shown in the shadow-graph. The present shock cell spacing agrees with that arising from the Prandtl-Pack shock cell spacing relation (Pack, 1950). As the distance of the strongest optic intensities shows the distance between standing waves of the screech tone, the numerical value of 0.82 times of the shock cell spacing nearly coincides with the experimental result of 0.8 obtained by Panda (1999).

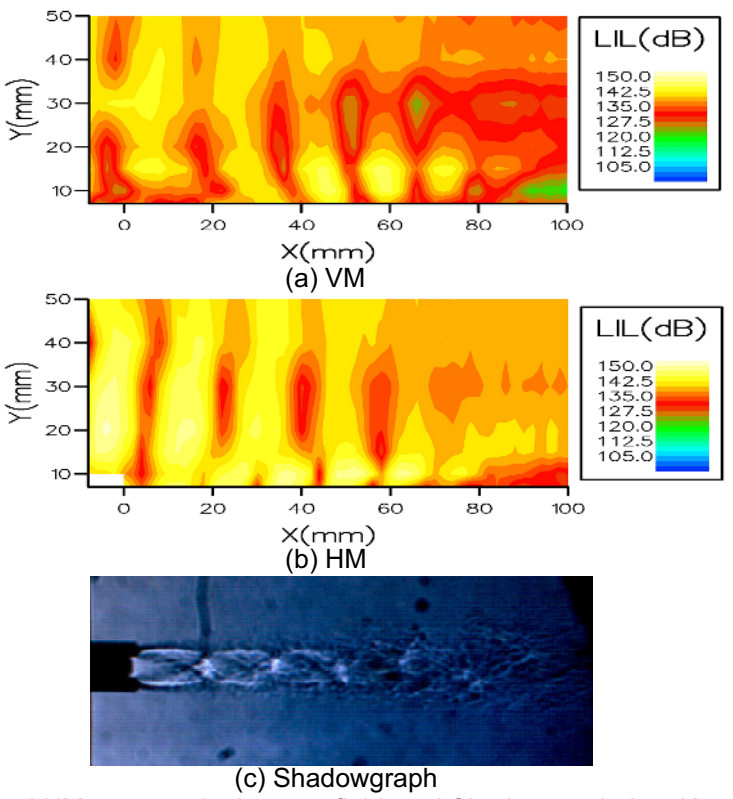


(a) VM

(b) HM

(c) Shadowgraph

Fig. 11. VM and HM contours in the near field, and Shadowgraph, L = 10 mm, f = 11 kHz.

Contours of laser signal intensity at a screech frequency of 11 kHz and a shadowgraph for L = 10 mm are shown in Fig. 11. From the figure of VM mode, the strongest sound source is located at the position near the 3rd and 4th shock waves as the same with the results of the plateless nozzle. The screech tone is intensified upstream by the reflector, and is decreased downstream. The sound generated influences on the jet structure. The velocity distributions along the jet center axis for the nozzle with the reflector of L = 10 mm decay earlier that of the nozzles with other reflector positions by a stronger acoustic wave. The sound field of the under-expanded jet doesn't show the axial-symmetrical features and changes to the acoustic characteristics of the flapping mode (Nakazono, 2006; Ono, 2007). About this mode transition, Kim (2003) stated that the flapping modes at lower jet Mach number are indicated as 'B' modes in Powell et al. (1992), where the plane of oscillation does not rotate about the jet axis, and the modes in the range of higher jet Mach number from 1.4 to 1.6 as 'D' modes, where the plane of oscillation rotates. If the flapping mode is B one, as the jet spreading differ at the vertical and the horizontal planes to the jet, the width of the sound wave between both planes may differ. Therefore, the laser intensity level obtained with the opt-microphone set at both planes may also differ. If the flapping mode is D one, the contours of the laser signal intensities will indicate the same one as the results shown in Fig. 11.

When seeing the figure of HM mode in Fig. 11, the stronger optic intensity at Y = 10 mm

distributes at the upside with a mean distance of every 13 mm. That is to say, the wavelength of the standing wave close to the jet is 13 mm. The wavelength of the standing wave at the position above Y = 20 mm becomes greater than that close to the jet. The wavelength is 17.7 mm and it is greater than a half wavelength of the sound wave. Moreover, the stronger sound intensity generated with this reflector-to-nozzle distance influences the jet flow, and it collapses the shock waves earlier. From the figure, we see the 3rd and 4th shock waves fluctuate in a lateral direction and the shock waves after the 5th shock wave are collapsed. Therefore, the velocity distribution on the jet center axis is also decayed earlier compared with that of the plateless nozzle.

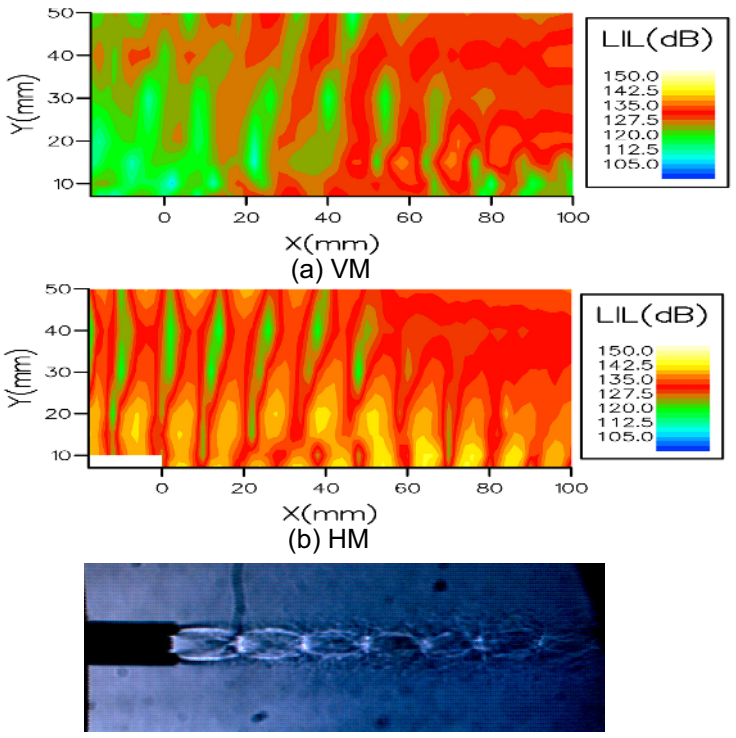


Fig. 12. VM and HM contours in the near field, and Shadowgraph, L = 20 mm, f = 15.1 kHz.

The contours of the laser signal intensity at a discrete frequency of 15.1 kHz and a shadowgraph for L = 20 mm are shown in Fig. 12. In the case of L = 20 mm, a discrete frequency of 12.5 kHz did not appear in the far field. However a sharp peak sound was seen at 15.1 kHz. For the position of L = 20 mm, the instability wave mode is considered to change, and then 15.1 kHz is adopted as a screech tone in the near field. From the contours of laser signal intensity for the VM mode in Fig. 9, the strongest optic intensity is located at the 3rd and 4th shock waves as the same as that of the plateless nozzle. The experimental facts indicate that the reflecting plate does not have an influence on the position of the strongest noise source. As well as this, from the shadow graphs the reflector does not also affect the spacing of shock waves. The relative intensive sound downstream is seen to propagate in the radial direction, and the sound near the plate is also weak in the case of the reflecting plate. When seeing the laser signal intensity contours of the HM mode, a strong opt-intensity close to the jet boundary is distributed at a spacing of every 10.5 mm from the upstream to the downstream. Above the radial distance of 20 mm, the strong optic intensity is located at an interval of every 11.8 mm. This interval is close approximately to a half wave length of the standing wave due to the reflection of the reflector.

From the above experimental results, the standing waves of the screech tone with the reflector differ at the place close to the jet boundary and the place a little far away toward the radial direction from the jet. Then, we consider the wave length at both places. The distance $L_{sw}$ between the two maximum in the standing wave pressure field set up by the hydrodynamic and acoustic pressure is given in the following equation.

$$\frac{1}{L_{sw}} = \frac{1}{\lambda_h} + \frac{1}{\lambda_s} \tag{2}$$

$$\frac{1}{L_{sw}} = \frac{f}{U_c} + \frac{f}{a} \tag{3}$$

where a is sound velocity, $\lambda$ wave length of the sound wave, f frequency of the sound wave, and $U_c$ convection velocity of instability wave, and the lower suffix h and s show the hydrodynamic and the sound respectively. Assuming the convection velocity is 0.7 times of jet velocity (Tam and Seiner, 1984), for the plateless nozzle, the wave length $L_{sw}$ of the calculated standing wave is 12.7 mm. It is found that the wave length of 12.3 mm measured for the HM mode nearly coincides with the calculated one. Then, we plot the screech tone frequencies at many places of the reflector from the nozzle as shown in Fig. 13(a). From the figure, it is found that the experimental data nearly agree with the values calculated by Eq. (3).

Next, we consider the wave length of the standing wave at the outside region of Y = 20 mm. In this range, the wave length is determined by the standing wave between sounds proceeding to and reflecting from the reflector. In the case of L = 10 mm, as the screech tone is a frequency of 11 kHz, its wave length $\lambda_a$ corresponds to 30.9 mm. Then, the calculated wave length of the standing wave, which corresponds to 15.45 mm, differs with the experimental data of 17.7 mm. Therefore, we assumed that the wave length of the standing wave is determined by the difference between the wave length of the sound wave and the wave length of the standing wave close to the jet, as shown in the following equation.

$$L_{20} = \lambda_a - L_{sw} \tag{4}$$

The obtained results are shown in Fig. 13(b). From the figure, the values calculated by Eq. (4) nearly agree with the experimental data.

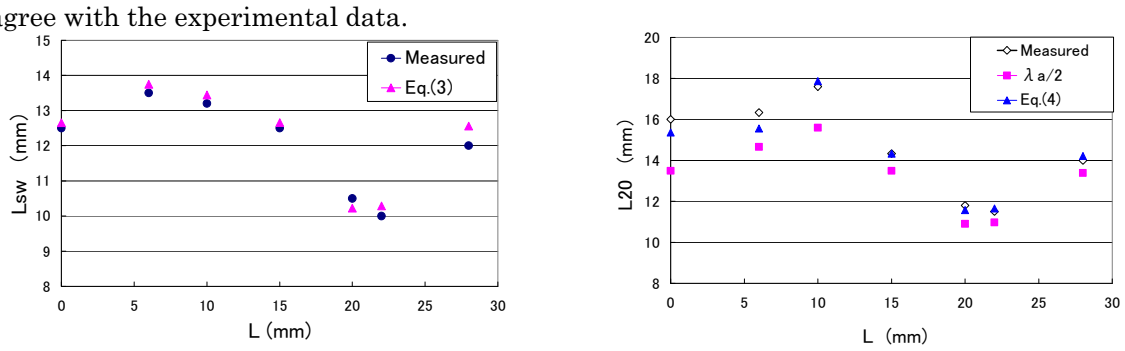


(a) Y = 10 mm (b) Y = 20 mm

Fig. 13. Wave length of standing wave as a function of reflector-to-nozzle spacing L.

# 5. Conclusions

The effect of the reflector on the near acoustic field of the screech jet has been studied using an opt-microphone.

1) The main noise source of the screech jet is placed near the 3rd and 4th shock locations, and its location is not influenced to a great extent by the reflector.
2) Screech tone does not have an influence on the spacing of the shock waves, but the maximum screech tone influences the jet and collapses the shock waves after the 5th shock wave.
3) The standing wave in the near field of the screech jet with the reflector has two types: One is the standing wave between the hydrodynamic pressure fluctuation propagating jet downstream and the sound pressure propagating upstream, and the other is the standing wave by the difference between the wavelength of the sound wave and the wavelength of the standing wave at the place close to the jet.

## *References*

Ahuja, K. K. and Massey, K. C., Flow/acoustic interaction in open-jet wind tunnels, AIAA Paper, 97-1691, (1997).
Evans, D. E. et al., Fourier optics approach to far forward scattering and related refractive index phenomena in laboratory plasmas, Plasma Phys. 24 (1982), 819-834.
Evans, D. E. et al., Measurement of long wavelength turbulence in a tokamak by extreme far forward scattering, Plasma Phys. 25 (1983), 617-640.

Harper-Bourne, M. and Fisher, M. J., The noise from shock waves in supersonic jets –Noise Mechanism-, AGARD CP-131, (1974), 11.1-11.13.
Kim, J. H. et al., Enhancement of Mixing in an underexpanded sonic round jet by an elliptic jet screech reflector, AIAA Paper, 2003-1274, ( 2003).
Nagel, R. T., Denham, J. W. and Papthanasiou, A. G., Supersonic jet screech tone cancellation, AIAA Journal, 21-11 (1983), 1541-1545.
Nakazono, Y. and Kosaka, M., Effect of notched nozzle geometry on the acoustic and flow characteristics of supersonic jets, Proceedings of the 11th International Symposium on Flow Visualization, F0064, (2002).
Nakazono, Y. and Sonoda, Y., Application of an optical wave microphone to Aerodynamic noise, Proceedings of the 8th Asian Symposium on Visualization, (2005), 11.1-6.
Nakazono, Y. and Kusuda, M., Effect of a hard reflector on supersonic jet screech tone, Journal of the Japan Society of Technology Education, 14 (2006), 37-43 (in Japanese).
Nakazono, Y., Kusuda, M., Sonoda, Y. et al., An optical wave microphone technique and its application to the measurement of jet noise, Proceedings of Inter-noise 2006, 625, (2006).
Norum, T. D., Screech suppression in supersonic jet, AIAA Journal, 21-2 (1983), 235-240.
Ono, N., Otomo, Y. and Koike, K., Behavior of underexpanded plasma jet in strong magnetic field, Journal of Visualization, 10-2 (2007), 227-236.
Pack, D. C., A note on Prandtl's formula for the wavelength of a supersonic gas jet, Q. J. Mech. Appl. Maths, Ⅲ (1950), 173-181.
Panda, J., An experimental investigation of screech noise generation, J. Fluid Mech., 378 (1999), 71-96.
Powell, A., On the mechanism of choked jet noise, Proc. Phys. Soc. Lond, 66 (1953), 313-327.
Powell, A. et al., Observations of the oscillation modes of choked circular jets, Journal of the Acoustical Society of America, 92-5 (1992), 2823-2836.
Ramesh, G., Venkatakrishnan, L. and Goubergrits, L., PIV studies of large scale structures in the near field of small aspect ratio elliptic jets, Journal of Visualization, 9-1 (2006), 23-30.
Rice, E. J. and Taghavi, R., Screech noise source structure of a supersonic rectangular jet, AIAA Paper, 92-0503 (1992).
Sonoda et al., Applications of the Fraunhofer diffraction method for plasma wave measurements, Plasma Phys. 25 (1983), 1113-1132.
Sonoda, Y. and Akazaki, M., Measurement of low-frequency ultrasonic waves by Fraunhofer diffraction, Jpn. J. Appl. Phys., 33 (1994), 3110-3114.
Sonoda, Y., Optical detection of sound waves and development of the optical wave microphone with no diaphragm, Proceedings of WESTPRA 7, (2001), 381-384.
Tam, C. K. W., Seiner, J. and Yu., J. C., On the relationship between broadband shock and screech tones, AIAA Paper, 84-2276 (1984).
Westley, R. and Wooley, J. H., The near field sound pressure of a choked jet when oscillating in the spinning mode, AIAA Paper, 75-479 (1975).

## *Authors Profile*

Yoichi Nakazono: He received his B.E., M.E. and D.E. degrees from Tokai University in 1971, 1973 and 1985. He works in Department of Mechanical Systems Engineering, School of Engineering, Kyushu Tokai University as a professor. His research interests are aero-acoustic and development of water musical instrument.

Yoshito Sonoda: He received his Ph.D. in Electrical Engineering in 1983 from Kyushu University. He works in Institute of Industrial Science and Technical Research, Kyushu Tokai University as a professor. His research interests are development of wave-optical sound detection method (optical wave microphone).

Yoshito Ohuchi : He received his B.E. M.E. and D.E. degrees from Kumamoto University in 1978, 1980 and 1996. He is now a Associate Professor in the Department of Information Systems, School of Engineering, Kyushu Tokai University. His research interests are new electronics circuits and computer simulations.

Yuki Nasu: He received his B.E. degree from Kyushu Tokai University in 2006. He is currently a graduate student in the Course of Production Engineering, Graduate School of Engineering, Kyushu Tokai University. His current research interests are noise reduction of supersonic jet noise and application of opt-microphone.